A Methodology for Engineering Design and Simulation of a Satellite Horn Antenna

Yoana Ivanova(✉) and Georgi Petrov

New Bulgarian University, 21 Montevideo Str., 1618 Sofia, Bulgaria
{yivanova,gpetrov}@nbu.bg

Abstract. This empirical research described in the paper aims to present applications of integrated technology solutions based on 3D modeling and simulation methods in satellite communications. The concept of the study is expressed in the proposed methodology related to conducting tests in several simulation environments in order to design functional prototypes. One of the main scientific and applied contributions of this methodology is considered to be the use of a 3D author's model of a pyramidal horn antenna for satellite communication.

In satellite communications and microwave applications, pyramidal horn antennas are used because of their UHF and SHF operational frequency ranges between 300 MHz and 30 GHz. They can be used as irradiators in lenticular and mirror antennas as well as an active element in dish antennas because they represent radiating structures built as extensions of standard rectangular waveguides in order to improve their directivity. The main requirements for an optimal system are maximum directivity and a minimum width of the radiation pattern, which is a graphical representation by a 2D or 3D diagram of the distribution of radiated energy into space, which is functionally dependent on the direction.

The assessment and analysis of the obtained results show that the simulation data of the preliminary tests is correct, which means that the 3D object is modeled precisely, verified and validated according to all requirements in the selected simulation systems.

Keywords: 3D and simulation modeling · 3D printing · satellite horn antenna

1 Introduction

Nowadays, antennas are mainly designed using electromagnetic 3D simulators, which provide an environment where a simulation 3D model of the antenna can be created in great detail and tested. In the antenna design process can be applied numerical techniques for electromagnetic analysis which are different compared to analytical ones as they are classified into integral methods (method of moments), differential methods (methods of finite differences and elements) and optical methods. *"The numerical simulation is performed in 3 steps: pre-processing, processing, and post-processing"* [1]. For example, the FDTD (Finite-Difference Time Domain) is a method of finite differences characterized by its capabilities for modeling nano-scale optical devices.

T. Zlateva and G. Tuparov (Eds.): CSECS 2023, LNICST 514, pp. 215–232, 2023.
https://doi.org/10.1007/978-3-031-44668-9_18

Therefore, the objective of the present research is to upgrade a previous author's experimental study (2004) realized by the software for horn and reflector analysis (Sabor). The basic scenario is realized by a parabolic mirror with a diameter between 50 and 100 cm irradiated by a planar antenna at a frequency of 2.45 GHz. The generated value of the gain is 33 dB. It should be noted that microstrip patches are planar structures which are used in microwave and radio frequency range.

The update of prior work is necessary due to some limitations of microstrip patches compared to other antenna types. For instance, they have a lesser gain than parabolic reflector antennas and are susceptible to interference from nearby objects and changes in the dielectric substrate's characteristics. Pyramidal horn antennas provide higher gain, better directivity, and a wider bandwidth. It is significant to note that pyramidal horn antennas have lower sidelobes, which means that interference from undesirable directions can be effectively reduced. Therefore, the primary focus of this study is on the modeling and simulation of pyramidal horn antennas.

Practically, the essence of the methodology proposed in the article is shown in Fig. 1 and presented in Sects. 2 and 3. In Sect. 2, the main concept of the current experiment is described. It is realized by using an engineering 3D model of a pyramidal horn antenna with dimensions generated in a Horn Antenna Calculator [2] and visualized by using an Easy RF Calculator that generates a horn antenna radiation pattern at the selected frequency [3]. The simulation study continues with a verification of the 3D model in the simulation product CST Studio Suite 2022. The implementation of the modeling process in Autodesk 123D Design is described in Sect. 3.

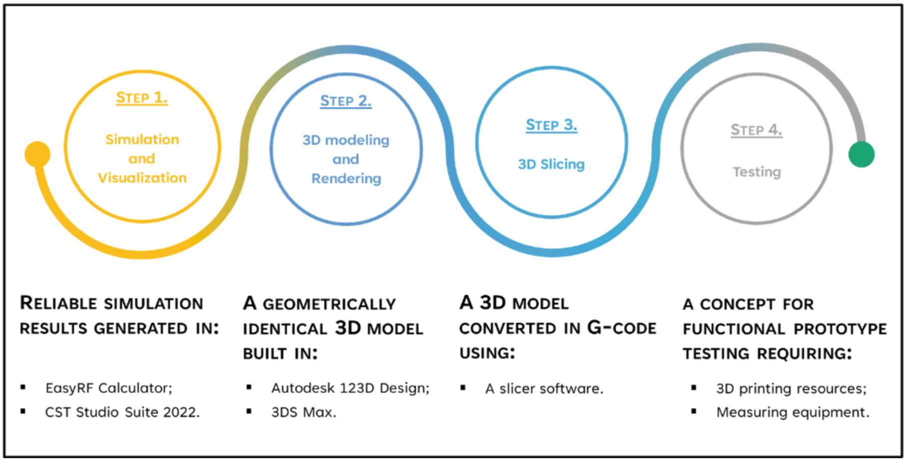

Fig. 1. A methodology for engineering design and simulation of a satellite horn antenna.

2 Simulations of the Radiation Pattern of the Pyramidal Horn Antenna

2.1 Calculating a Pyramidal Horn Antenna

There are different types of rectangular horn antennas depending on the direction of flaring [4].

- *sectoral horn antennas* – they are characterized by one-directional flaring. *"If this flaring is in the direction of an electrical vector, it is called a sectoral E-plane horn antenna, and if the flaring is in the direction of a magnetic vector, then it is called a sectoral H-plane horn antenna".*
- *pyramidal horn antennas* – its *"flaring is done in the electrical as well as magnetic vector of the rectangular waveguide".* One of the main characteristics of these antennas is the emitting opening called aperture (A), which must meet the requirement of being at least twice as large as the waveguide. The formulas for the A_E (L_E - slant length of the side in the E-field direction) and A_H (L_H - the slant length of the side in the H-field direction) are [5]:

$$A_E = \sqrt{2\lambda L_E} \tag{1}$$

$$A_H = \sqrt{3\lambda L_H.} \tag{2}$$

The effective aperture A_{Eff} depends on the optimal gain G, as follows:

$$A_{Eff} = \frac{G\lambda^2}{4\pi} \tag{3}$$

Due to these specifics, it is necessary to make some assumptions before starting the simulation study:

- *in the simulation environment, the antenna can be considered as an ideal lossless device, which means that the gain (G) is equal to the directivity (Dir., D);*
- *in a physical environment $G < D$.*

Table 1 includes the results generated by the calculators used. In Figs. 2, 3, and 4, screenshots from EasyRF Calculator for the three selected frequencies are shown. The reference planes for linearly polarized antennas, E-plane (the electric field) and H-plane (the magnetizing field) are orthogonal to each other: Phi = 90° (E-plane) and Phi = 0° (H-plane). Unlike the strongest "mainlobe" in the center, "sidelobes" can radiate in other directions, which is not desirable [6]. The electric field vector can be denoted by E_y and is drawn in red, while the magnetic field vectors H_x and H_z are drawn, respectively, in blue and green.

Table 1. A comparison of the results generated in the Horn Antenna and EasyRF Calculators.

Antennas	f, GHz	AxB, mm	G, dBi Horn Antenna Calculator	D, dBi EasyRF Calculator
A_1	8	61.5 × 41	12	19.56
A_2	4	123 × 82	12	13.80
A_3	2	246 × 164	12	7.98

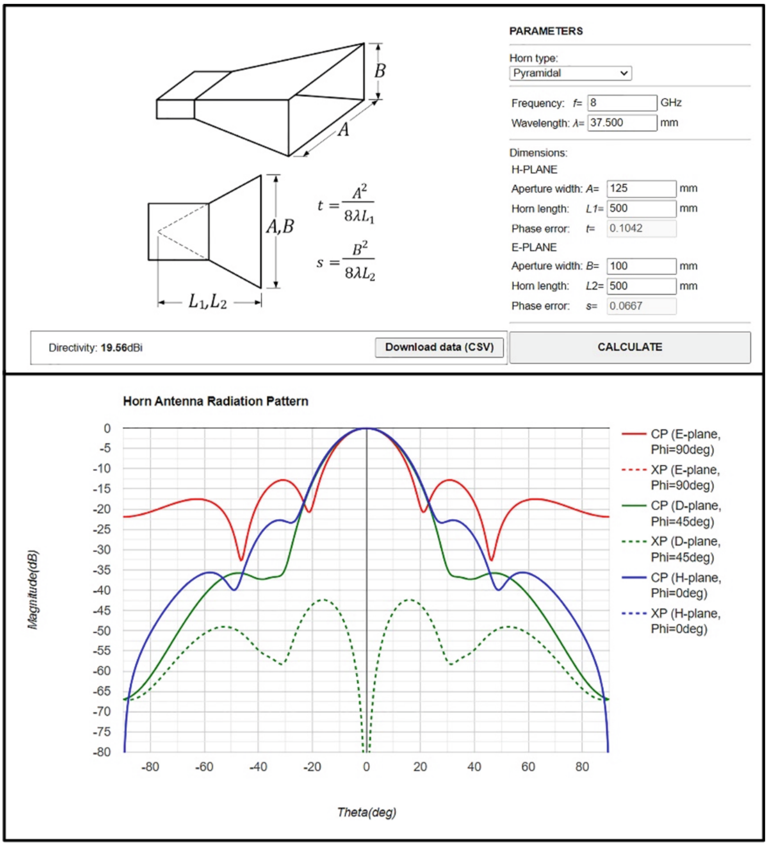

Fig. 2. The pyramidal horn antenna radiation pattern at f = 8 GHz.

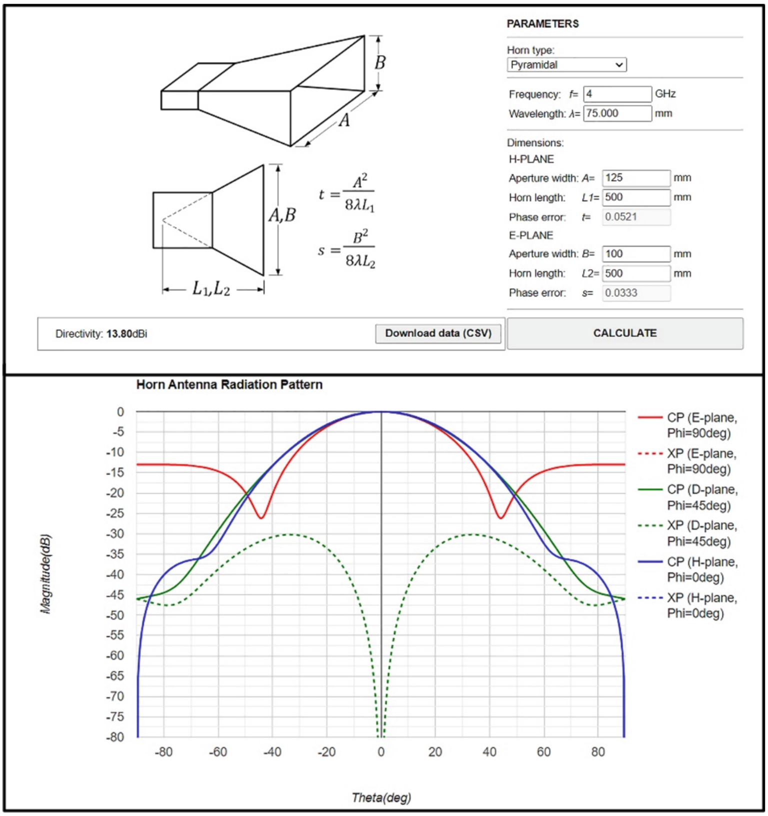

Fig. 3. The pyramidal horn antenna radiation pattern at f = 4 GHz.

Actually, the FDTD method solves Maxwell's equations at discrete points on a mesh in time and space to simulate wave propagation. It *"computes E and H at grid points spaced Δx, Δy, and Δz apart, with E and H interlaced in all three spatial dimensions. FDTD includes the effects of scattering, transmission, reflection, absorption, etc."* [7, 8]. The Maxwell – Heaviside equations represent differential equations that are expressed mathematically as follows:

$$\nabla \cdot \mathrm{D} = \rho_{\mathrm{v}} \tag{4}$$

$$\nabla \cdot \mathrm{B} = 0 \tag{5}$$

$$\nabla \times \mathrm{E} = -\frac{\partial B}{\partial t} \tag{6}$$

$$\nabla \times \mathrm{H} = j + \frac{\partial D}{\partial t} \tag{7}$$

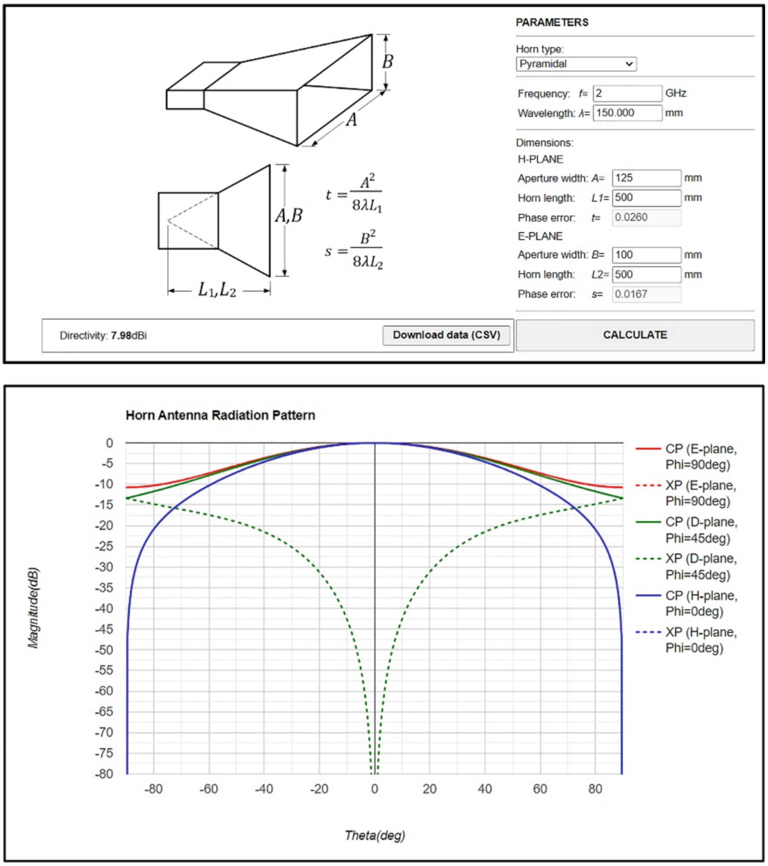

Fig. 4. The pyramidal horn antenna radiation pattern at f = 2 GHz.

In the Eqs. 4 and 5 are accepted the following designations:

- *electric flux density (D) – the propagation of the electric field (E) through a medium with permittivity (ε):*

$$D = \varepsilon E \tag{8}$$

- *magnetic flux density (B) - the propagation of the magnetic field (H) through a medium with permeability (μ):*

$$B = \mu H \tag{9}$$

- *charge density (ρv) describes the distribution of the charge within the medium.*
- *current density (j) - describes the distribution of current within the medium.*

After applying the curl operator to both sides of Eq. 6, the obtained result is as follows:

$$\nabla \cdot \nabla \times E = -\nabla \frac{\partial \times B}{\partial t} \tag{10}$$

$$\nabla^2\mathrm{E} = -\nabla\frac{\partial \times \mu H}{\partial t} \tag{11}$$

$$\nabla \times \mathrm{H} = j + \frac{\partial D}{\partial t} = j + \frac{\partial \varepsilon \mathrm{E}}{\partial \mathrm{t}} \tag{12}$$

$$\nabla^2\mathrm{E} = \frac{\mu\varepsilon\partial^2\mathrm{E}}{\partial t^2} \tag{13}$$

$$\nabla^2\mathrm{E} = \frac{\partial^2\mathrm{E}}{\partial x^2} + \frac{\partial^2\mathrm{E}}{\partial y^2} + \frac{\partial^2\mathrm{E}}{\partial y^2} \tag{14}$$

Obviously, the percentage error is smallest for A_2 – 13% assuming the true value is generated in the EasyRF Calculator and 15% otherwise. It is calculated by the following formula:

$$\mathrm{Error} = \frac{\mathrm{V_o} - \mathrm{V_t}}{\mathrm{V_t}}, \tag{15}$$

where *Error* is the percentage error, V_o is the observed value, and V_t is the true value.

2.2 A Verification of the Simulation 3D Model of a Pyramidal Horn Antenna

As it can be seen in Table 2, the values of the gain in the EasyRF Calculator are about 1.5 times higher compared to those generated in CST Studio Suite 2022. In Fig. 5 and 6 the farfield radiation patterns at 4 and 2 GHz are shown. The farfield radiation directivity diagrams at 8, 4, and 2 GHz are shown respectively in Figs. 7, 8, and 9 depending on the angle “Phi” that measures the angular distance to the x-axis in the lateral plane, while the angle “Theta” measures the angular distance from the pole that is situated in the z-direction. These angles are defined in the “Spherical Coordinate System”, which means that “for a Cartesian vector (x, y, z) of length r, the angles can be obtained by the following relations [9]:

$$\varphi = arctan\frac{y}{x} \tag{16}$$

$$\theta = arccos\frac{z}{r} \tag{17}$$

Table 2. A comparison of the results generated in EasyRF Calculator and CST Studio Suite.

Antennas	f, GHz	A × B, mm	D, dBi EasyRF Calculator	D, dBi CST Studio Suite
A_1	8	61.5 × 41	19.56	12.51
A_2	4	123 × 82	13.80	7.825
A_3	2	246 × 164	7.98	5.399

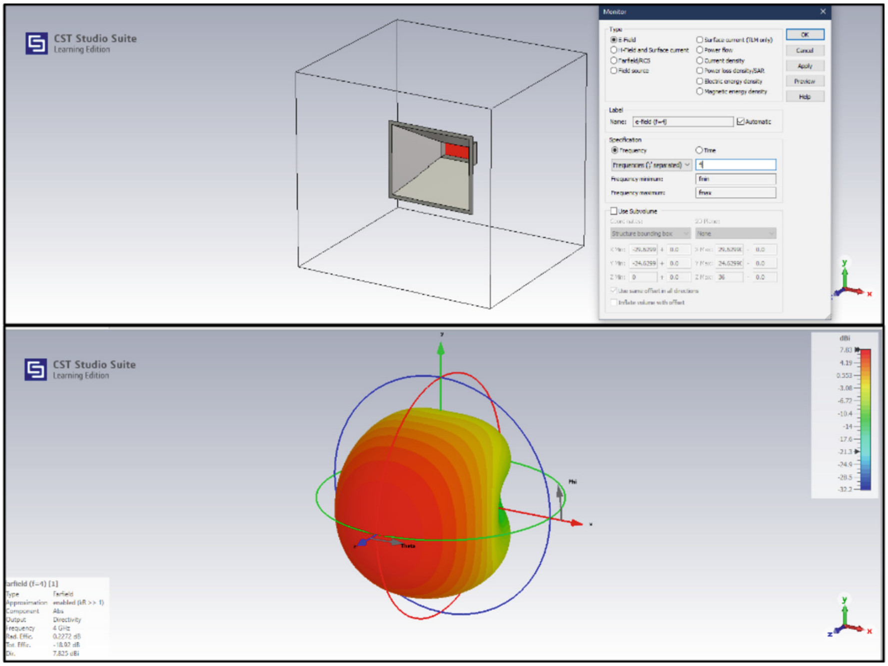

Fig. 5. The pyramidal horn antenna radiation pattern at f = 4 GHz.

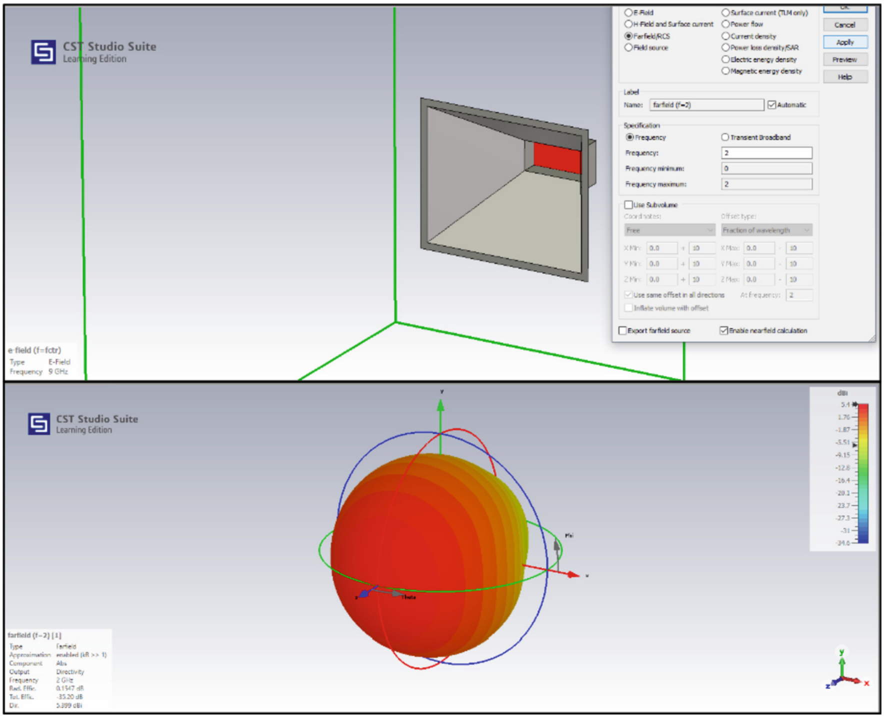

Fig. 6. The pyramidal horn antenna radiation pattern at f = 2 GHz.

2.3 Assessment and Analysis of the Simulation Results

In order to evaluate and analyze the simulation results, directivity diagrams and radiation patterns from previous studies by author[1] *("Excitation sources of a mirror antenna for wireless Internet", 2004)* are applied for comparison to illustrate the progress of the visualizations of the simulation results (Figs. 10 and 11). It can be concluded that, despite the high quality of the 3D visualizations generated in Zeland IE3D and Sabor, the possibility to import a 3D model of a radio engineering device into the simulation environment is an advantage in terms of clarity.

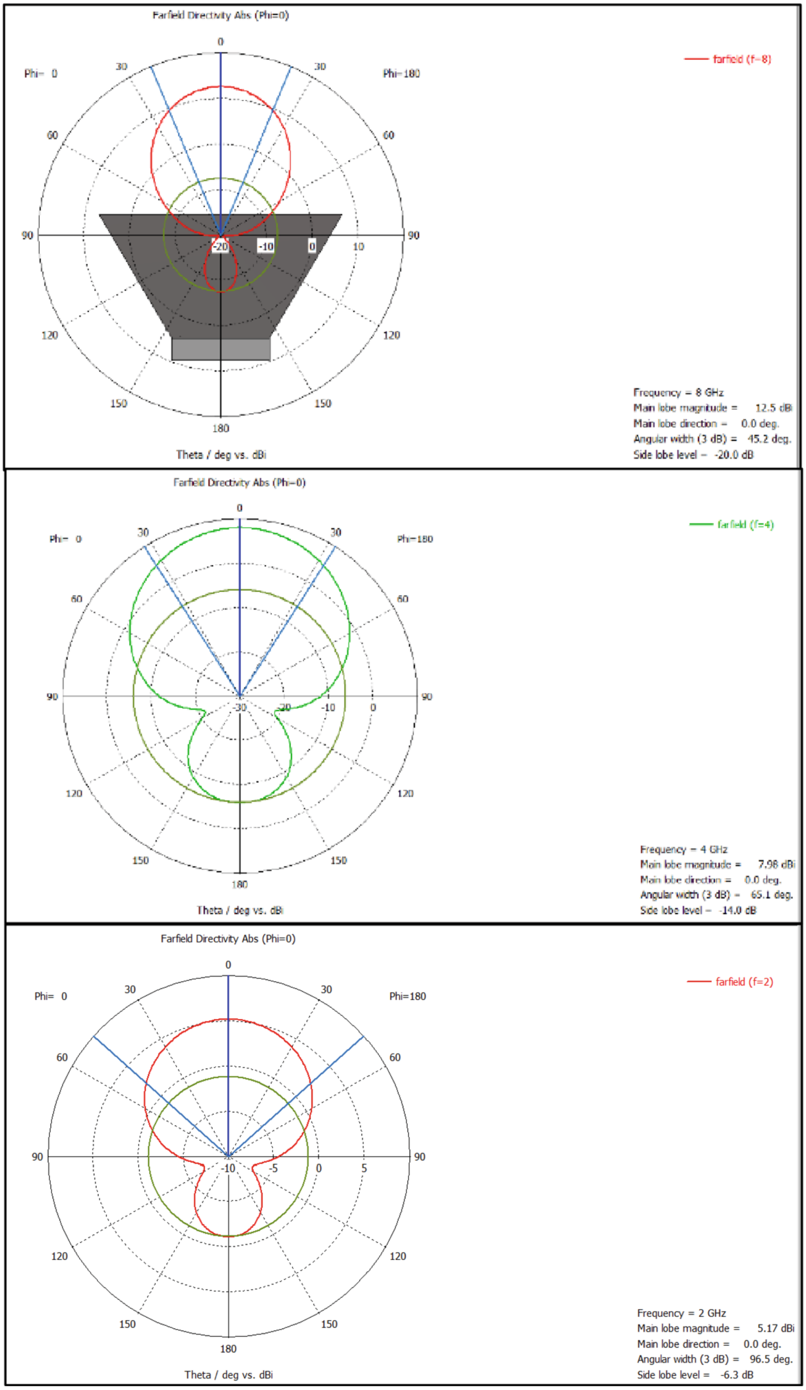

Fig. 7. The farfield radiation directivity diagrams at Phi = 0° and f = 8, 4, and 2 GHz.

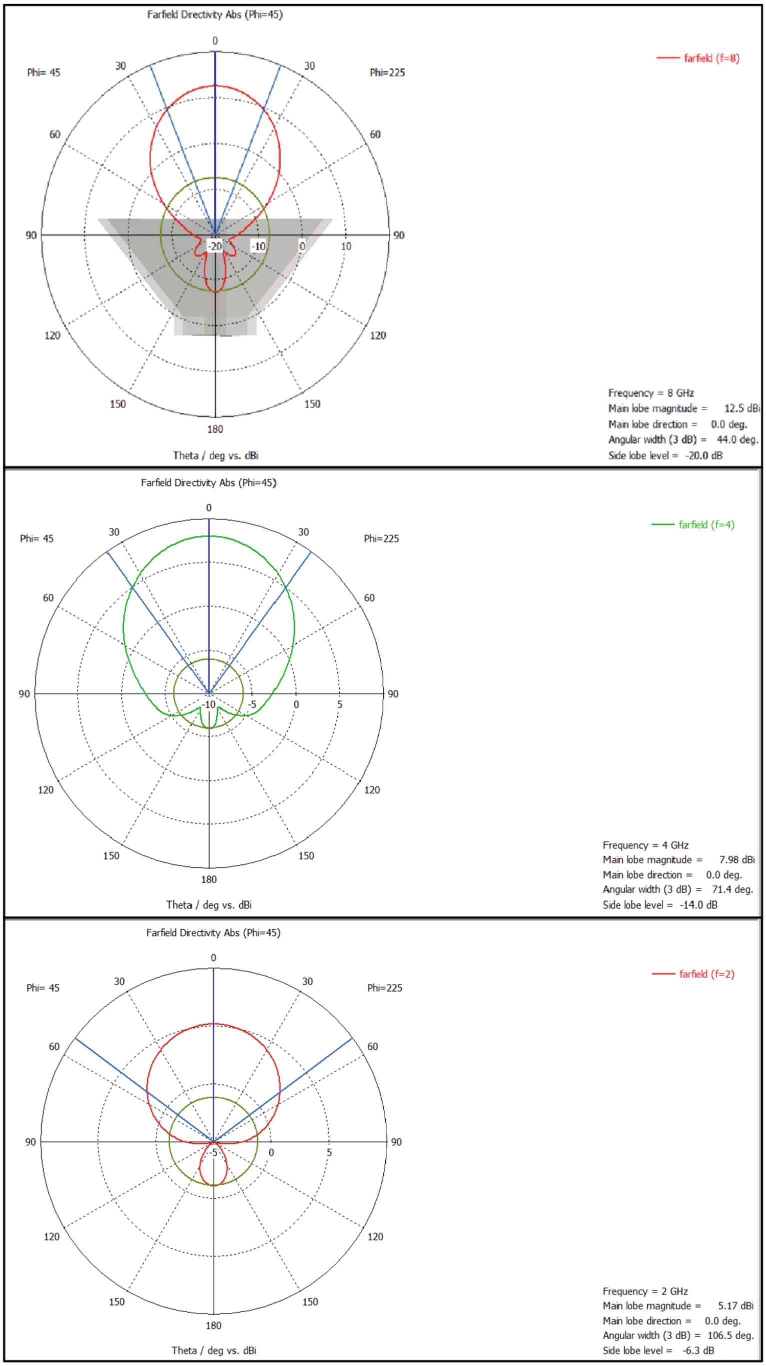

Fig. 8. The farfield radiation directivity diagrams at Phi = 45° and f = 8, 4, and 2 GHz.

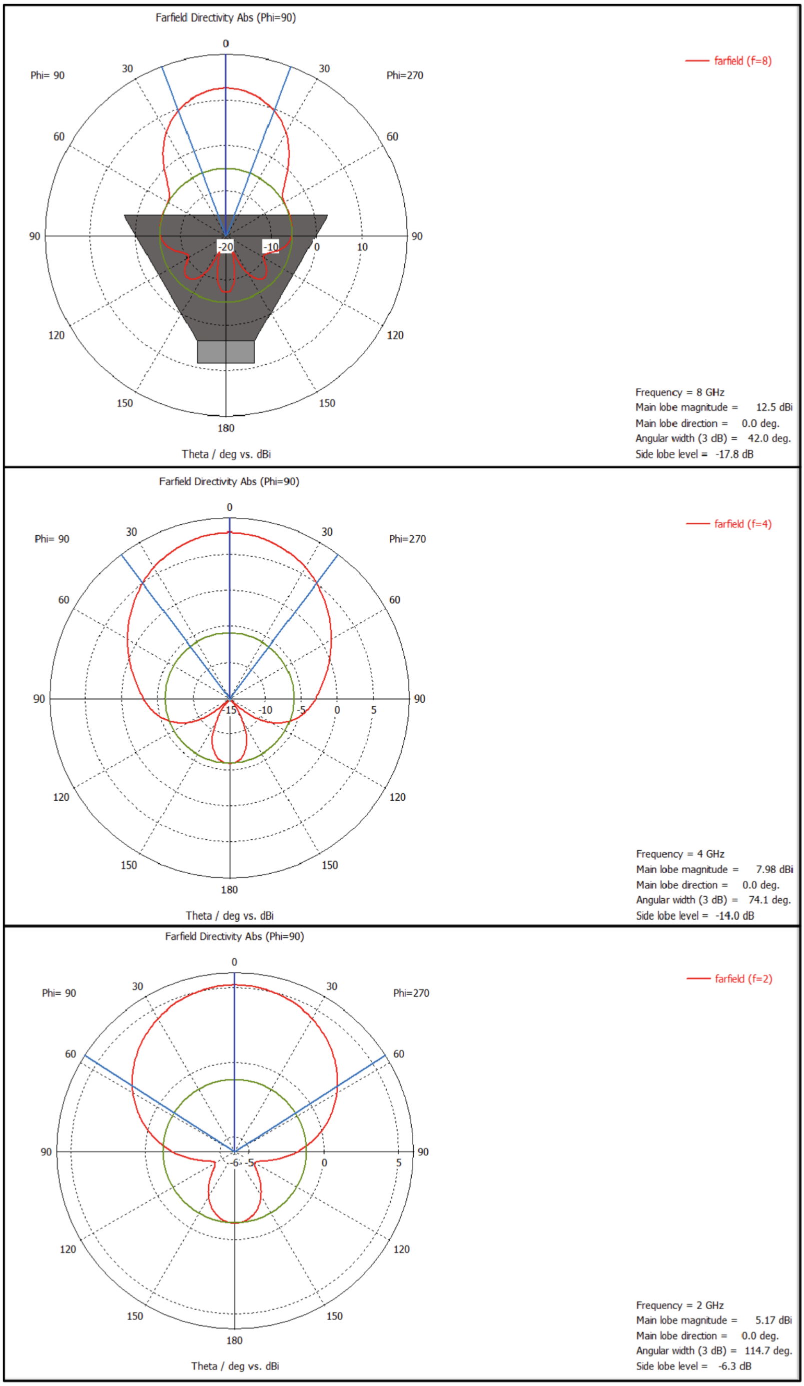

Fig. 9. The farfield radiation directivity diagrams at Phi = 90° and f = 8, 4, and 2 GHz.

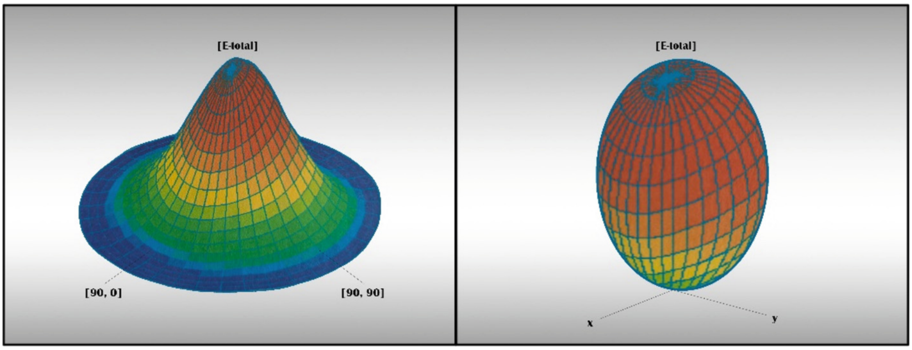

Fig. 10. Radiation patterns generated in Zeland IE3D at f = 2.45 GHz

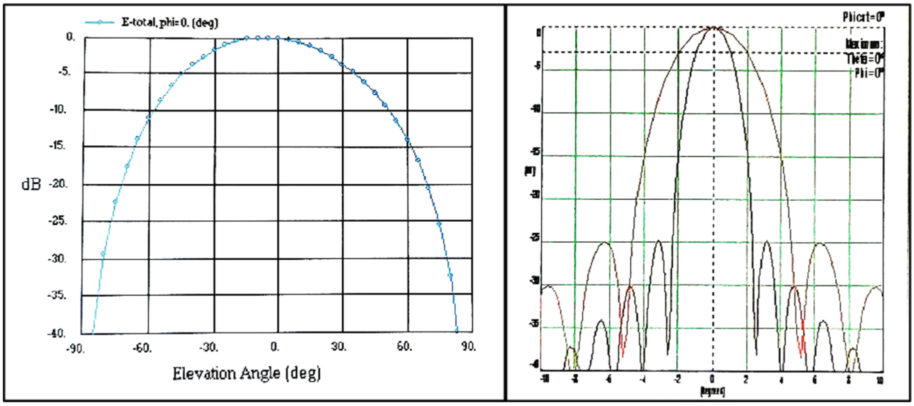

Fig. 11. Directivity diagrams generated in Zeland IE3D and Sabor at f = 2.45 GHz

3 3D Modeling of a Functional Prototype of a Pyramidal Horn Antenna

3.1 3D Modeling Methods

The author's 3D model is created by the method of solid modeling following the steps and by the tools in Table 3 using software for engineering modeling Autodesk 123D Design, with the dimensions generated in the Horn Antenna Calculator at 8 GHz simulated and visualized using a "macros" 3D model in CST Studio Suite 2022 as it is described in Sect. 2. Some examples of 3D visualizations generated in the simulator are shown in Fig. 12 to illustrate the advantage of using 3D computer graphics in engineering and science in order to achieve greater clarity and informativeness of output data.

Actually, 3D models can be imported into simulation environments for conducting additional tests for the purposes of a detailed comparison analysis with the results obtained in item 2.2 of Sect. 2. In regard to practical 3D modeling, the first algorithm is recommended as more direct, while the second could be determined as more complex

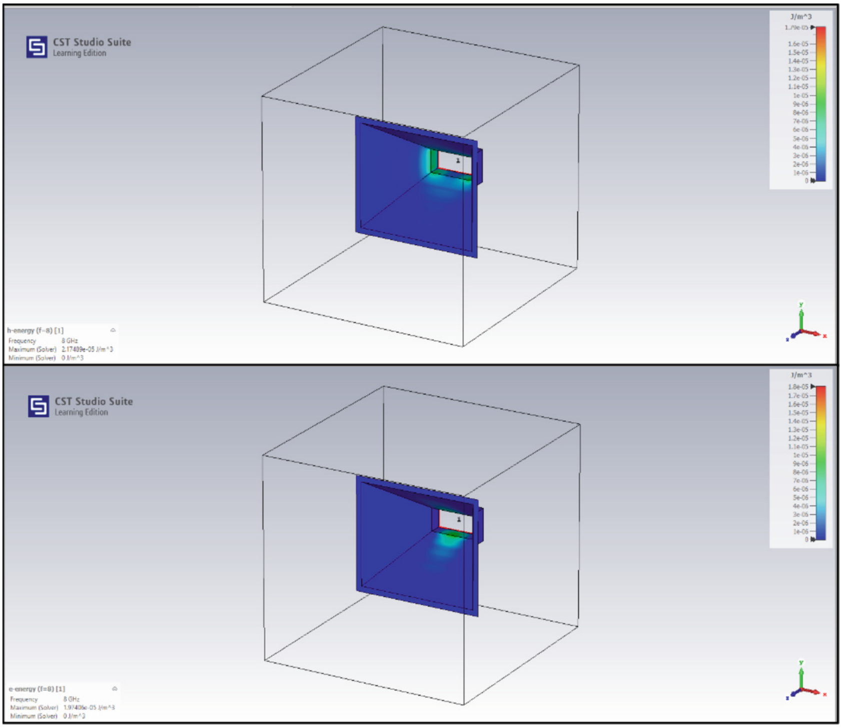

Fig. 12. Visualizations using a 3D model of a pyramidal horn antenna in CST Studio Suite 2022 at f = 8 GHz: e-energy; h-energy.

but suitable for some particular situations of difficulties related to possible input parameter limitations of some tools like "Shell", which defines the thickness of the antenna's wall.

Table 3. Algorithms for 3D modeling of a pyramidal horn antenna in Autodesk 123D Design.

Solid Modeling	Groups of Tools	3D Modeling Algorithm
Method 1	Construct, Modify, Transform	Primitive Box > Smart Scale > Sketch: Rectangle > Transform: Measure > Transform: Align > Construct: Loft > Modify: Shell
Method 2	Construct, Modify, Combine, Transform	Primitive Box > Smart Scale > Transform: Align > Clone > Combine: Subtract > Tweak > Sketch: Rectangle > Construct: Extrude > Delete

Rendered images of the model with a different metal material applied in Autodesk 123D Design and 3DS Max are shown in Fig. 13 to compare the level of visual realism. In fact, the main advantage of Autodesk 123D Design is the capability for precise engineering modeling, while the quality of visualization looks high in 3DS Max.

3.2 A Concept for Testing 3D Printed Functional Prototypes of a Satellite Horn Antenna

The model of a pyramidal horn antenna can be 3D printed and used for testing using conventional and compatible physical devices. Before the printing process, the model must be sliced in a slicer software like PrusaSlicer, Lychee, Cura, XYZ Print, etc. Regardless of the printing technology (FDM - Fused Deposition Modeling used for 0.9–2.4 GHz, SLS- Selective Laser Sintering for frequencies above 1.3 GHz), in all cases, additional manual processing of the final products is required, considering smoothing the working surfaces of the antennas or additional varnishing of the products with a UV protective layer. Both types of materials require coating the working surfaces and all contact interface areas with a metallized layer of silver zinc paint or by vacuum metallizing the products.

The use of semi-transparent materials allows the creation of multi-colored products that can be used in teaching students, thus making it possible to see the working surfaces and elements of the antenna inside, even making a gradual colorization of the working surfaces show the intensity of the electromagnetic fields (EMF) inside the antenna. The proposed methodology can be applied not only to antennas but also to the production of larger microwave systems using waveguides with very complex architectures.

It should be noted that applications of such systems must be used carefully because 3D printed technology using different types of plastics can reduce the lifecycle of systems because of material degradation over time, deformations because of higher working temperatures, and sudden failures of components because of lower temperatures. The superiority achieved by this technology is mainly associated with the possibility to make spare parts or to design and test highly complex waveguide systems, as well as the lower price of the final product compared to classic metallic products. Particular attention should be paid to the creation of products that are designed to fly or work in vacuum space due to the presence of voids and microcracks.

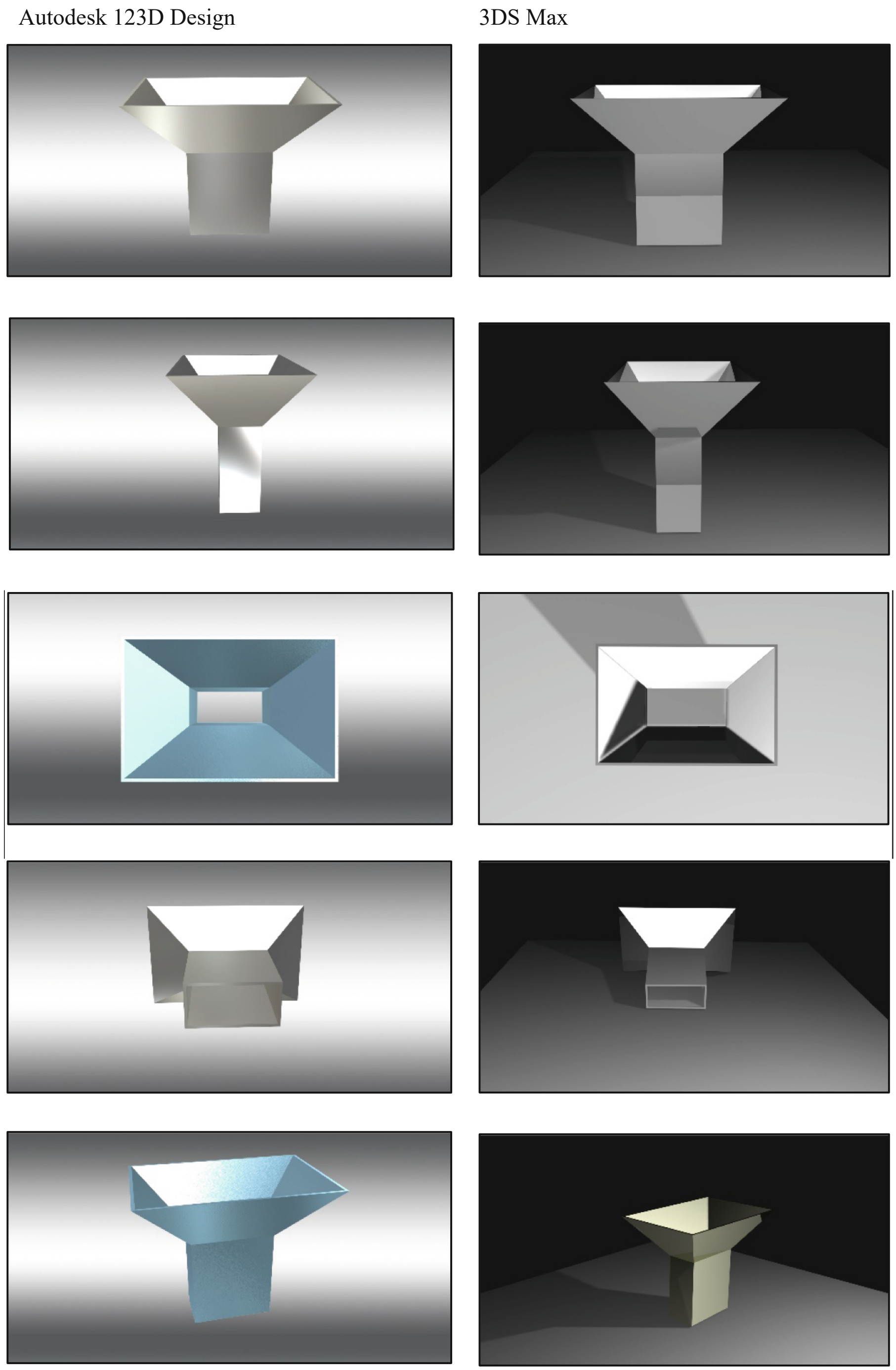

Fig. 13. Rendered images of the 3D model of a pyramidal horn antenna with a metal material applied.

4 Conclusion

In conclusion, it can be summarized that the completion of all the steps in the proposed methodology ensures reliable results and qualitative visualizations in simulation environments, while the 3D modeling products provide highly realistic rendering and can be combined successfully to achieve professional results. The contemporary design with CAD/CAM and 3D printing of radio engineering devices is a high-tech area providing innovative technologies that contribute to serial machine production at the stages of precise engineering modeling, manufacturing, and testing functional prototypes.

This research can be continued by 3D printing the model from different materials (PLA and PETG) after a pre-printing preparation. In addition, the proper selection of 3D printing resources (filaments and 3D printers) is important to improve the quality of the functional prototypes, which can be used to conduct experimental research with measuring physical devices [10]. Conducting experiments in laboratory conditions can be not only very effective and productive but also related to methods for the investigation of EMF [11, 12] as well as innovative solutions for the prevention of electromagnetic radiation from mobile radio transmitting stations [13] and gamming attacks.

References

1. Dankov, P.: Anteni za mobilni i satelitni komunikatsii, prilozhenia za ustanovyavane na mestopolozhenie, GPS-sistemi. In: Conference: Lyatno uchilishte za uchiteli “Fizika za i sas smartfon”, 11–15 yuli, FzF na SU “Sv. Kliment Ohridski”, Sofia (2016)
2. Kustarev, V.: Horn Antenna online calculator, (2015–2022). https://3g-aerial.ben/online-calculations/antenna-calculations/horn-antenna-online-calculator. Accessed 15 May 2023
3. EasyRF. https://hornantennacalculator.blogspot.com/p/calculator.html. Accessed 15 May 2023
4. Meena, M., Prakash, V.: Simulation results of rectangular horn antenna. Int. J. Eng. Technol. **3**(1), 171–179 (2018)
5. Electronics Notes. Microwave Horn Antenna Theory. https://www.electronics-notes.com/articles/antennas-propagation/horn-antenna/theory-equations.php. Accessed 21 May 2023
6. Dankov, P.: Microwave measurement of electrical fields in different media – principles, methods and instrumentation. J. Phys: Conf. Ser. **516**(1), 012001 (2014)
7. David, D.S.K., Jeong, Y., Wu, Y.C., Ham, S.: An analytical antenna modeling of electromagnetic wave propagation in inhomogeneous media using FDTD: a comprehensive study. Sensors **23**(8), 3896 (2023). https://doi.org/10.3390/s23083896
8. SYNOPSYS, Finite-Difference Time-Domain Method. https://www.synopsys.com/glossary/what-is-fdtd.html#C. Accessed 21 May 2023
9. Farfield Calculation Overview. https://space.mit.edu/RADIO/CST_online/mergedProjects/3D/special_postpr/special_postpr_pp_farfield.htm
10. Pasarelski R., Pasarelska, T.: Metodika za izsledvane i analiz na radiotehnicheski prametri na universalni mobilni telekomunikatsionni sistemi, Sbornik nauchni trudove ot godishna nauchna konferentsia s mezhdunarodno uchastie na natsionalen voenen universitet “Vasil Levski” – Veliko Tarnovo (2013)
11. Stancheva, A., Tzvetkov, P., Mihova, P.: International research projects - justification for introduction of lower exposure limits for EMF with low intensity, CD “Godishnik, tom 1” 2014. Departament Zdraveopazvane i sotsialna rabota, NBU, Sofia (2014). ISSN 1313-7875

12. Stancheva, A., Pasarelski, R., Kadrev, V.: Metodi za namalyavane na radiosmushteniyata v LTE mrezhi. Sbornik dokladi ot godishna universitetska nauchna konferentsia, pp. 670–677, Natsionalen voenen universitet “Vasil Levski”, V.Tarnovo (2017). ISSN 2367-7481
13. Pasarelski, R., Stancheva, A., Tsvetkov, P.: Mehanizmi za preventsia ot elektromagnitno izlachvane ot mobilni radiopredavatelni stantsii. In: Sbornik dokladi na XXVI Mezhdunaroden nauchen simpozium s mezhdunarodno uchastie „Metrologia i metrologichno osiguryavane2016, Sozopol, Bulgaria, pp. 383–392 (2016). ISSN 1313-9126